INFLUENCE OF EXTERNAL TURBULENCE ON THE VELOCITY FIELD IN THE WAKE BEHIND AN ELLIPSOID OF REVOLUTION

B. A. Kolovandin and N. N. Luchko

UDC 532.517.4

The velocity field in the wake behind an ellipsoid of revolution is numerically investigated on the basis of a second-order differential model as a function of the energetic and structural state of the external isotropic turbulence.

The most important characteristic of a turbulent velocity field is the turbulent Reynolds number $R_\lambda = q\lambda/\nu$, $q^2 = \overline{u_i' u_i'}$, $\lambda = \sqrt{5\nu q^2/\varepsilon_u}$, $\varepsilon_u = \nu\overline{(\partial u_i'/\partial x_k)^2}$. The quantity R_λ varies in a broad range of values in the majority of turbulent flows. The simplest example of such a situation is the degeneration of homogeneous isotropic turbulence behind a cascade. The energy damping rate of the fluctuating motion here depends in a substantial manner on the quantity R_λ. Indeed, in the initial developed degeneration domain where $R_\lambda \gg 1$ a law with exponent $n = -1.3$ is valid [1], while the final stage ($R_\lambda < 1$) is characterized by the exponent $n = -2.5$ [2].

As a rule, numerical computations of turbulent inhomogeneous velocity fields are conducted at this time on the basis of asymptotic models ($R_\lambda \gg 1$) $\overline{u_i' u_j'} - \varepsilon_u$ with a known set [3] of empirical constants. It is shown in [4-7] that the empirical constants must be replaced by functions of the turbulent Reynolds number in the analysis of turbulence parameters in the domain of continuous change in R_λ from large values to small, corresponding to the final stage of degeneration.

SECOND-ORDER DIFFERENTIAL MODEL

The closed system of average equations describing the turbulent velocity field of a shear flow consists of equations for the mean velocities $\bar{U}_i$, the Reynolds stresses $\overline{u_i' u_j'}$ and the dissipation functions ε_u:

$$\frac{\partial \bar{U}_i}{\partial x_i} = 0; \quad \bar{U}_k \frac{\partial \bar{U}_i}{\partial x_k} = -\frac{1}{\rho}\frac{\partial \bar{P}}{\partial x_i} + \frac{\partial}{\partial x_j}\left(\nu \frac{\partial \bar{U}_i}{\partial x_j} - \overline{u_i' u_j'}\right);$$

$$\bar{U}_k \frac{\partial \overline{u_i' u_j'}}{\partial x_k} - P_{ij} - \alpha \frac{\partial}{\partial x_k}\left[\frac{q^4}{\varepsilon_u}\left(\frac{\partial \overline{u_i' u_j'}}{\partial x_k} + \frac{\partial \overline{u_i' u_k'}}{\partial x_j} + \frac{\partial \overline{u_j' u_k'}}{\partial x_i}\right)\right] + \gamma_u\left(P_{ij} - P_{ii}\frac{\delta_{ij}}{3}\right) + \alpha \frac{\partial}{\partial x_i}\left(\frac{q^4}{\varepsilon_u}\frac{\overline{u_j' u_k'}}{\partial x_k}\right) +$$

$$+ \alpha \frac{\partial}{\partial x_j}\left(\frac{q^4}{\varepsilon_u}\frac{\partial \overline{u_i' u_k'}}{\partial x_k}\right) + a_u \varepsilon_u \left(\frac{\overline{u_i' u_j'}}{q^2} - \frac{\delta_{ij}}{3}\right) + 2\left[d_u \frac{\overline{u_i' u_j'}}{q^2} + (1 - d_u)\frac{\delta_{ij}}{3}\right]\varepsilon_u - \nu \frac{\partial^2 \overline{u_i' u_j'}}{\partial x_k^2} = 0;$$

$$\bar{U}_k \frac{\partial \varepsilon_u}{\partial x_k} - b_u \frac{\varepsilon_u}{q^2}\overline{u_i' u_k'}\frac{\partial \bar{U}_i}{\partial x_k} - \beta \frac{\partial}{\partial x_i}\left(\frac{q^2}{\varepsilon_u}\overline{u_i' u_k'}\frac{\partial \varepsilon_u}{\partial x_k}\right) - F_u \frac{\varepsilon_u^2}{q^2} - \nu \frac{\partial^2 \varepsilon_u}{\partial x_k^2} = 0;$$

$$P_{ij} = -\overline{u_i' u_k'}\frac{\partial \bar{U}_j}{\partial x_k} - \overline{u_j' u_k'}\frac{\partial \bar{U}_i}{\partial x_k}; \quad d_u = \frac{\delta}{(R_\lambda + \sqrt{R_\lambda^2 + \delta})^2};$$

$$F_u = \frac{11}{3} - \frac{13}{15} d_u; \quad b_u = 2{,}9(1 - d_u) + 2{,}45 d_u; \quad \delta = 2.8 \cdot 10^3; \quad a_u = 5{,}6(1 - d_u); \quad \gamma_u = 0{,}475(1 - d_u).$$

The model takes account of the dependence of the empirical parameters on the turbulent Reynolds number and does not contradict the exact regularities of the dynamics of a homogeneous isotropic field in the asymptotic cases $R_\lambda \to \infty$ [8] and $R_\lambda \to 0$ [9]. In the domain of moderate values of R_λ the form taken for the function $d_u(R_\lambda)$ is hypothetical in nature. The functions F_u, b_u, a_u, γ_u are constructed with the results of direct numerical modeling in the domain of moderate numbers R_λ [10, 11], and experimental data on the dynamics of homogeneous

A. V. Lykov Institute of Heat and Mass Transfer, Academy of Sciences of the Belorussian SSR, Minsk. Translated from Inzhenerno-Fizicheskii Zhurnal, Vol. 48, No. 4, pp. 538-546, April, 1985. Original article submitted December 15, 1983.

 0022-0841/85/4804-0390$09.50

turbulence with constant shear [12] taken into account. Values of the empirical constants $\alpha = 0.0375$ and $\beta = 0.075$ are determined by numerical optimization from the condition of best agreement of the results of computation and experiment for different free flows.

FORMULATION OF THE PROBLEM

The stationary turbulent velocity field in the wake behind an axisymmetric body is modeled by the system of equations (1) written in a cylindrical coordinate system in the boundary-layer approximation. Eliminated from consideration here is the domain directly behind the body for which the transport equations are not suitable in the boundary-layer approximation.

Using the ellipsoid diameter d and the free stream velocity U_∞ as characteristic parameters and introducing the notation $x = x_1/d$, $r = x_2/d$, $u = (\bar{U}_1 - U_\infty)/U_\infty$, $v = \bar{U}_2/U_\infty$, $R_{ij} = u'_i u'_j/U_\infty^2$, $E = R_{ii}$, $R = R_{12}/r$, $D_u = \varepsilon_u d/U_\infty$, it is easy to write the system of equations in dimensionless form

$$\frac{\partial ur}{\partial x} + \frac{\partial vr}{\partial r} = 0;$$

$$(1+u)\frac{\partial R}{\partial x} + v\frac{\partial R}{\partial r} = \frac{1}{r}\frac{\partial}{\partial r}\left(r\nu_E\frac{\partial R}{\partial r}\right) + \frac{2\nu_E}{r}\frac{\partial R}{\partial r} - \frac{1-\gamma_u}{r}R_{22}\frac{\partial u}{\partial r} - 2\rho_u\frac{D_u}{E}R; \tag{2}$$

$$(1+u)\frac{\partial R_{22}}{\partial x} + v\frac{\partial R_{22}}{\partial r} = \frac{1}{r}\frac{\partial}{\partial r}\left(r\nu_E\frac{\partial R_{22}}{\partial r}\right) - \frac{2(1-\rho_u)}{3}D_u - 2\rho_u D_u\frac{R_{22}}{E} - \frac{2}{3}\gamma_u rR\frac{\partial u}{\partial r};$$

$$(1+u)\frac{\partial E}{\partial x} + v\frac{\partial E}{\partial r} = \frac{1}{r}\frac{\partial}{\partial r}\left(r\nu_E\frac{\partial E}{\partial r}\right) - 2rR\frac{\partial u}{\partial r} - 2D_u;$$

$$(1+u)\frac{\partial D_u}{\partial x} + v\frac{\partial D_u}{\partial r} = \frac{1}{r}\frac{\partial}{\partial r}\left(r\nu_\varepsilon\frac{\partial D_u}{\partial r}\right) - b_u\frac{D_u}{E}rR\frac{\partial u}{\partial r} - F_u\frac{D_u^2}{E};$$

$$\nu_E = \frac{1}{RE} + \alpha\frac{E^2}{D_u}; \quad RE = \frac{U_\infty d}{\nu}; \quad \nu_\varepsilon = \frac{1}{RE} + \beta\frac{ER_{22}}{D_u};$$

$$\rho_u = d_u + 2{,}8(1-d_u).$$

The radial component of the mean velocity vanishes on the axis of symmetry, while the remaining functions evidently have zero derivatives. The quantities $E(x, \delta)$ and $D_u(x, \delta)$ are determined by the energetic and structural state of the free-stream turbulence, assumed homogeneous and isotropic, on the outer boundary δ; therefore, $R_{22}(x, \delta) = {}^1/_3 E(x, \delta)$, $u(x, \delta) = R(x, \delta) = 0$. The boundary δ itself is found from the condition of a smooth connection between the computed characteristics of the wake and the background.

Six possible background states are considered whose parameters $x = 3$ and $r \geq \delta$ are represented in Table 1. In the case of degenerating external turbulence the boundary conditions for $x \geq 3$ are determined by the solution of the Cauchy problem for the system

$$\frac{dE_b}{dx} = -2D_{ub}; \quad \frac{dD_{ub}}{dx} = -F_u\frac{D_{ub}^2}{E_b}. \tag{3}$$

If the background is stationary, then the conditions $D_u(x, \delta) = D_{ub}$ and $E(x, \delta) = E_b$ contradict system (1). In this case the right sides of the equations for R_{22}, E, and D_u are supplemented, respectively, by the source terms $2D_{ub}/3$, $2Du_{ub}$, $F_u D_{ub} D_u/E$ that model the generator of the background turbulent fluctuations and assure stationarity conditions (independence from x) for the external turbulence.

The background intensity in all the versions under consideration does not exceed 0.05% of the turbulence energy on the axis of symmetry in the section $x = 3$, and, therefore, its influence on the initial conditions can be neglected.

The first version characterizes the external flow with rapidly degenerating turbulence whose intensity is negligible compared with the turbulence energy along the axis of symmetry at any distance from the ellipsoid, which corresponds to the development of a wake in an unperturbed stream. The five succeeding versions model the influence of the energetic, structural, and dynamic states of the external, isotropic turbulence on the development of the remote axisymmetric wake.

TABLE 1. Characteristic External Isotropic Turbulence Parameters for x = 3

No. of version	E_b	L_b	$R_{\lambda b}$	External turbulence
1	10^{-6}	0,25	2,24	Degenerating
2	10^{-6}	50	31,62	»
3	10^{-6}	500	316,2	»
4	10^{-6}	5,56	10,55	Stationary
5	10^{-6}	50	31,62	»
6	$81 \cdot 10^{-6}$	5,56	31,62	»

NUMERICAL INTEGRATION METHOD

The passage to the system of algebraic equations for the mesh functions is realized by using a two-layer six-point Krank–Nicholson scheme that approximates the differential operators in the half-integer points with an error $o(\Delta r^2 + \Delta x^2)$. The linearized system of algebraic equations was solved by the scalar factorization method [13]. The iterative process was continued until the maximum difference in the magnitude of the turbulence energy between two successive iterations was less than 0.1% of the value of E on the axis of symmetry.

A uniform spacing along the radius with $N_0 = 50$ nodes is given in the initial section. As we proceed downstream, the number of nodes in the transverse section grows; when it was twice the initial value, the spacing Δr was doubled. The longitudinal spacing was given by a linear function of the distance behind the ellipsoid $\Delta x = \alpha x + b$. The number of nodes across the layer and the parameters $\alpha = 0.0025$ and $b = 40$ were determined as a result of a numerical experiment with a different magnitude of the spacings Δr and Δx in the sections $3 \leq x \leq 10^2$ and $10^4 \leq x \leq 10^5$.

COMPARISON BETWEEN THE RESULTS OF THE COMPUTATION AND A LABORATORY EXPERIMENT

Comparison between the computed and experimental [14] profiles for $5 \leq x \leq 70$ shows their good agreement for a defect in the mean velocity u and the second moments R_{ij} in both the transverse and longitudinal coordinates, but indicates a significant discrepancy between the results being compared for the dissipation function D_u in both quantitative and qualitative respects. Represented in Fig. 1 in the section x = 40 are the computed profile of D_u and the experimental [14]: isotropic $D_{uo} = 15D_{11}$, $D_{ij} = \nu(\partial u'_i/\partial x_j)^2$ and partially taking account of the influence of anisotropy of the profile D_{uc}. The function D_{uc} is calculated on the basis of five measured components of the dissipation tensor (D_{11}, D_{12}, D_{13}, D_{21}, D_{31}) while isotropic approximations were used for the remaining components $D_{22} = D_{12}/2$, $D_{23} = D_{13}$, $D_{32} = D_{12}$, $D_{33} = D_{13}/2$. As follows from Fig. 1, as the number of measured components of the dissipation tensor increases, the difference between the computation and experiment diminishes somewhat. An analogous situation is observed in each of the sections under consideration. Let us note that the known experimental results [15-17] on the distribution of D_u in the transverse section of axisymmetric coflows indicate agreement between the point of maximum D_u and the axis of symmetry while it is shifted toward the domain of greatest gradient in the mean velocity in the computation (Lumley and Khajch–Nouri [18] obtained an analogous result). The disagreement noted between the numerical and experimental data on the distribution of D_u is apparently explained both by the large errors in measuring the total dissipation and by the insufficiently adequate modeling of the vorticity generation process in the turbulent shear flow.

WAKE DEVELOPMENT IN AN UNPERTURBED FREE STREAM

The numerical computation is executed in the section $3 \leq x \leq 10^6$ of longitudinal coordinate variation where the turbulent Reynolds number calculated along the axis of symmetry diminishes monotonically to the value 0.05. In addition to the parameters evaluatable directly because of the solution of the system (1) of differential equations, the scale of turbulence is of considerable interest. If the quantities E and D_u are known, then the problem of determining the characteristic scale of turbulence is easily solvable only in the limit cases $R_\lambda \to \infty$ and $R_\lambda \to 0$, where the standard scales are, respectively, the scale of the energy-containing vortices $L = 5E\sqrt{E}/D_u$ and the microscale λ. Let us introduce the parameter $\Lambda = L/(1 -$

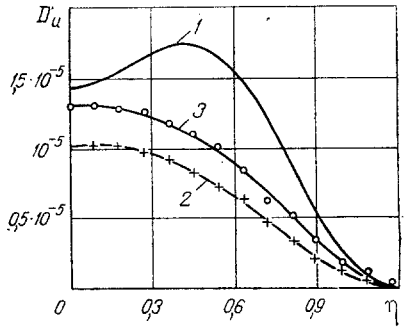

Fig. 1

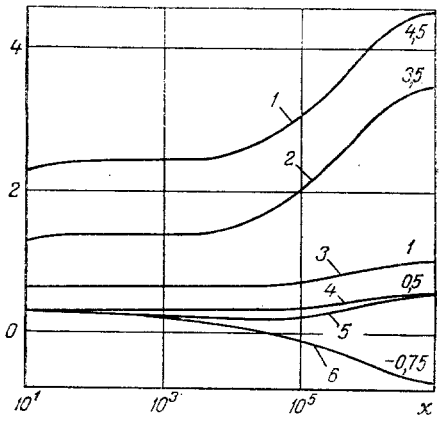

Fig. 2

Fig. 1. Radial profiles of the turbulence kinetic energy dissipation rate in the section x = 40 (computed 1; experimental 2: 2) D_{uo}, and 3) D_{uc}).

Fig. 2. Dependence of the power-law exponents on the longitudinal coordinate: 1) nD; 2) nE; 3) nu; 4) nΛ; 5) nδ; 6) nL.

d_u) into the analysis. It is easy to see that in the domain of strong turbulence where $d_u \to 0$, the quantities L and Λ agree. In the case $R_\lambda \to 0$, the function d_u is proportional to R_λ; consequently, the scales Λ and $\lambda = L/R_\lambda$ are also proportionate in the weak turbulence domain. Qualitatively, the dependence of Λ on R_λ is in agreement with the dependence of the integral scale $\Lambda = q^{-2}\int_0^\infty \overline{u_i' u_i'}(\xi)\xi_k^2 d\xi$ on the turbulent Reynolds number. Therefore, the scale Λ can be used as a characteristic quantity for arbitrary values of the number R_λ. The evolution of each of the computed turbulent wake characteristics along the axis of symmetry was approximated by the power law dependences: $u(x, 0) = A_u(x + x_o)^{-nu}$, $E(x, 0) = A_E(x + x_o)^{-uE}$, $L(x, 0) = A_L(x + x_o)^{nL}$, etc. (the dependence of the exponent on the longitudinal coordinate is evidently a necessary condition for self-similarity). The magnitude of the radius on which the energy $E(\delta_E)$ is one-quarter of its value on the axis of symmetry was used as the geometric parameter of the width of the wake.

Analysis of the computation results permits noticing a number of features in the development of an axisymmetric wake in an unperturbed stream.

1. As follows from Fig. 2, two self-similarity zones can be extracted during degeneration of an axisymmetric wake: the near, corresponding to the strong turbulence domain and governed by large values of R_λ, and the far which occurs for $R_\lambda < 1$.

2. In the far self-similarity zone, the "weak" turbulence does not influence the defect in the mean velocity (Fig. 2), which degenerates according to the law x^{-1} as in the laminar flow case. Because of the insignificant average shear the fluctuating motion energy is not generated here while the total effect of the diffusion and dissipation assures its rapid attenuation with exponent nE = 3.5. The width of the wake δ_E or δ_u (governed by the defect in the mean velocity) and the scales Λ and λ are mutually proportional and grow with the exponent n = 0.5. The scale of the energy-containing vortices here decreases as $x^{-0.75}$, remaining less than λ and losing the physical meaning of a characteristic length scale. Therefore, far self-similarity is characterized by two velocity scales (u and $\sqrt{E}$) and one length scale λ. Let us note that the results of a computation on the evolution of the far wake are in complete agreement with the Phillips analytical laws [19]. (The magnitude of the exponents in the Phillips asymptotic power laws is noted by the numbers in Fig. 2.)

3. The turbulent velocity field in the near self-similar domain is characterized by one velocity and length scale ($\sqrt{E}$ and L).

4. The near and far self-similar zones differ not only by the magnitude of the damping exponent but also of the self-similar profile shapes, as follows from Fig. 3.

5. The diminution in the value of R_λ downstream influences the deviation of the damping rate of the characteristics being computed from the self-similar strong turbulence laws to a different degree. While the exponent nu remains practically constant down to $R_\lambda = 10$, the

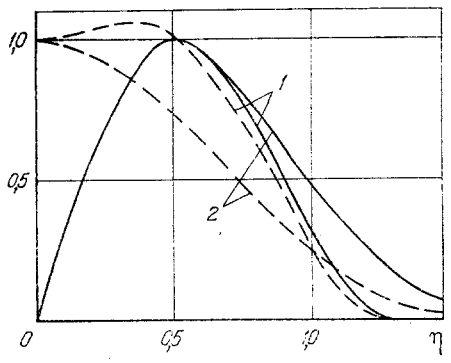

Fig. 3

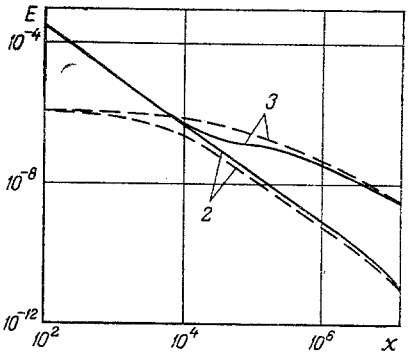

Fig. 4

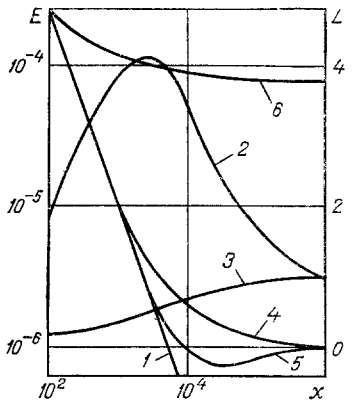

Fig. 5

Fig. 3. Turbulent energy (dashed line) and tangential stress (solid line) distributions across the wake: 1) x = 100; 2) 10^6.

Fig. 4. Damping of turbulence kinetic energy along the wake axis of symmetry (solid lines) and in the free stream (dashes): 2, 3) version number.

Fig. 5. Influence of the external stationary turbulence on the scale and turbulence energy evolution along the wake axis of symmetry: 1) E_1; 2) L_4/L_b; 3) L_5/L_b; 4) E_4; 5) E_5; 6) E_6.

the quantity nL diminishes noticeably starting with $R_\lambda = 30$. The ratio $L/\lambda = R_\lambda$ here decreases rapidly, indicating a diminution in the range of vortex sizes present in the wake zone.

6. The passage of the turbulent velocity field from the strong to the weak state of turbulence is a slow non-self-similar process. The significant removal of the far self-similarity zone from the body explains the reason for the Freymuth lack of success [20] in trying to verify the Phillips law experimentally behind a sphere for $R_\lambda = 2.4$.

WAKE INTERACTION WITH DEGENERATING EXTERNAL TURBULENCE

For a given isotropic background intensity in the initial section, its rate of degeneration is determined by the magnitude of the length scale of the energy-containing vortices L. In the case of a relatively large-scale and weakly intensive external flow (version 2), its turbulence degenerates considerably more slowly than the turbulence energy along the axis of wake symmetry. As is seen from Fig. 4, as the longitudinal coordinate increases, equilibration of the inertia of turbulence occurs on the wake axis and in the external flow, but a certain excess of the intensity E_2 above E_b for $x > 2 \cdot 10^4$ is explained by turbulent energy generation in the wake because of the mean velocity gradient. At a sufficiently large distance behind the body, wake evolution is governed entirely by the regularities of external turbulence (background) degeneration and is, in principle, different from the wake dynamics in an unperturbed stream (for the same longitudinal coordinate values). The possibility of such a situation must be taken into account in interpreting a laboratory experiment investigat-

ing the far wake behind a body in a wind tunnel where degenerating isotropic turbulence is realized as a rule.

An important result in principle is obtained as the background length scale L_b increases further in the initial section (version 3). Still slower damping than in version 2 occurs here for the background turbulence intensity, and the process of interaction between turbulent flows of different scales, i.e., by the wake and the free stream, is weakened. In such case, a situation occurs when the background and wake intensity are equilibrated at a certain distance from the ellipsoid (curves E_3 and E_{b3}), but the influence of the background has still not reached the wake axis where the value of the length scale L remains less than in the background. Consequently, the relative fine-scale wake turbulence degenerates at a higher rate and its intensity becomes less than in the background. As the longitudinal coordinate increases further, the influence of the background reaches the axis of symmetry, the difference in the values of the scale L on the wake axis and in the background diminishes, and equilibration occurs of the wake and external flow turbulence intensities.

FEATURES OF WAKE INTERACTION WITH NONDEGENERATE EXTERNAL TURBULENCE

Analysis of the nature of energy damping of the fluctuating motion along the wake axis of symmetry for versions 1 and 4-6 (E_1 and E_4-E_6, respectively, Fig. 5) permits extraction of a number of features of wake development in a nondegenerate turbulent stream.

1. As the external flow turbulence intensity increases beyond the dependence on its structural state, the distance at which the influence of the background reaches the axis of symmetry diminishes.

2. For identical energetic and different structural states of the external turbulence (versions 4 and 5), a diminution in the scale L_b results in magnification of the background influence on wake development. As for the degenerating large-scale background, a situation can occur for the case of stationary external turbulence with sufficiently large values of L_b when the intensity of the relatively fine-scale turbulence in the wake during downstream motion along the axis of symmetry will take on values less than E_b in this section. When the influence of the background reaches the axis of symmetry, the turbulence energy on the wake axis grows monotonically and tends to its asymptotic value E_b.

3. For an identical dynamic state of the external flow, the relatively fine-scale and highly intensive external turbulence (version 6) exerts considerably greater influence on wake development than does the weakly intensive and fine-scale background.

4. The influence of an isotropic turbulent background on the central part of the wake is manifest in a rapid diminution of the tangential stress $\overline{u'_1u'_2}$. Consequently, the defect in the mean velocity damps out far downstream according to the law x^{-1}, as in the laminar case although the value of the turbulent Reynolds number here is still not small.

NOTATION

R_λ, turbulent Reynolds number; q^2, doubled kinetic energy of turbulent velocity fluctuations; λ, Taylor length scale; ν, kinematic viscosity coefficient; ε_u, dissipation rate; x_i, Cartesian coordinates; L, Kolmogorov length scale; Λ, integral scale of turbulence; d_u, b_u, F_u, empirical functions of the Reynolds number; α, β, δ, empirical constants; x, r, dimensionless cylindrical coordinates; U_∞, free stream velocity; d, characteristic diameter of the ellipsoid of revolution; u, defect in the mean velocity; E, doubled dimensionless fluctuation energy; R_{ij}, dimensionless second moments; D_u, dimensionless dissipation rate; nu, nE, nδ, nD, nL, nΛ, exponents in the self-similar laws; δ_E, δ_u, wake half-widths; $\eta = r/\delta_E$, self-similar transverse coordinate.

LITERATURE CITED

1. G. Compte-Bellot and S. Corrsin, "The use of contraction to improve the isotropy of grid-generated turbulence," J. Fluid Mech., 25, 657-682 (1966).
2. J. C. Bennet and S. Corrsin, "Small Reynolds number nearly isotropic turbulence in a straight duct and a contraction," Phys. Fluids, 21, 2129-2142 (1978).
3. W. Frost and T. H. Moulden (eds.), Handbook of Turbulence, Plenum Press, New York—London (1977).
4. B. A. Kolovandin and N. N. Luchko, "Numerical modeling of the turbulent velocity field

of an axisymmetric momentum-free wake," Heat and Mass Transfer-VI, Vol. 1, Pt. 2 [in Russian], Inst. Heat and Mass Transfer, Academy of Sciences of the Belorussian SSR, Minsk (1980), pp. 126-135.
5. B. A. Kolovandin, "On the question of modeling turbulence dynamics for its nonasymptotic state," Problems of Turbulent Transfer [in Russian], Inst. Heat and Mass Transfer, Beloruss. Acad. Sci., Minsk (1982), pp. 3-21.
6. B. A. Kolovandin, Modeling of Heat Transfer in Inhomogeneous Turbulence [in Russian], Nauka i Tekhnika, Minsk (1980).
7. B. A. Kolovandin, "Correlation modeling of transfer processes in shear turbulent flows," Preprint No. 5 [in Russian], Inst. Heat and Mass Transfer, Beloruss. Acad. Sci., Minsk (1982).
8. P. G. Saffman, "Note on decay of homogeneous turbulence," Phys. Fluids, 10, 1349-1357 (1967).
9. L. G. Loitsyanskii, "Certain fundamental regularities of isotropic turbulent flow," Trudy TsAGI, No. 440, 2-23 (1939).
10. J. R. Herring, "Statistical turbulence theory and turbulence phenomenology," NASA, SP-321, 41-46 (1973).
11. U. Schuman and G. S. Patterson, "Numerical study of pressure and velocity fluctuations in nearly isotropic turbulence," J. Fluid Mech., 88, 685-709 (1978).
12. F. H. Champagne, V. G. Harris, and S. Corrsin, "Experiments on nearly homogeneous shear flow," J. Fluid Mech., 41, 81-139 (1970).
13. A. A. Samarskii, Introduction to the Theory of Difference Schemes [in Russian], Nauka, Moscow (1971).
14. B. A. Kolovandin, N. N. Luchko, Yu. M. Dmitrenko, and V. L. Zhdanov, "Turbulent wake behind an axisymmetric body and its interaction with external turbulence," Preprint No. 10 [in Russian], Inst. Heat and Mass Transfer, Beloruss. Acad. Sci., Minsk (1982).
15. M. S. Uberoi and P. Freymuth, "Turbulent energy balance and spectra of the axisymmetric wake," Phys. Fluids, 13, 2205-2210 (1970).
16. V. I. Bukreev, V. A. Kostomakha, and Yu. M. Lytkin, "Axisymmetric turbulent wake behind streamlined body," Dynamics of a Continuous Medium [in Russian], No. 10, Hydrodynamics Inst. Siberian Branch, USSR Acad. Sci., Novosibirsk (1972), pp. 202-207.
17. I. Wygnanski and R. Fiedler, "Some measurements in the self-preserved jet," J. Fluid Mech., 38, 577-612 (1966).
18. J. L. Lumley and M. Khajch-Nouri, "Computational modeling of turbulent transport," Adv. Geophys., 18A, 169-193 (1974).
19. O. M. Phillips, "The final period of decay of nonhomogeneous turbulence," Proc. Camb. Philos. Soc., 52, 135-151 (1955).
20. P. Freymuth, "Search for the final period of decay of axisymmetric turbulent wake," J. Fluid Mech., 68, 813-839 (1975).